

Simulation of Particle Trajectory of 1.8-in Hard Disk Drive

Sikarin Jintranun¹ and Kiatfa Tangchaichi²

ABSTRACT

A simulation of the particle trajectory of a 1.8-in hard disk drive is constructed based on precise actual dimensions of a current 1.8-in hard disk drive in the market with 3600 rpm rotation speed. The RNG k -epsilon model is used to investigate the air flow in the hard disk drive. The general particle trajectory has been calculated using the discreet random walk model (stochastic tracking). In the model, 0.5 μ -in particles have been released from the top of the Head Stack Assembly (HSA) bearing, the particles are brought inward to the centre of the rotating disk then they are thrown outward toward the disk edge closer to the disk surface. The particles barely move to the coil side of the HSA because the air velocity is lower than inside the rotating disk area. Also the whirl of the air at the ramp load area creates a spiral like trajectory.

INTRODUCTION

The emergence of 1.8-in hard disk drives in the consumer electronic device market has pushed the usage of this new form of hard disk drive. At the same time, hard disk manufacturing continues to enhance the capacity and the speed of hard disk drives. One of the biggest concerns is Track Miss Registration (TMR) which is caused by air flow in the hard disk drive. This concern still remains in this new form factor.

Investigations of airflow in HDD reported in recent year were studies of 2.5-in, 3.5-in and 1-in HDD (M.A. Suriadi et al., 2006) (Albert Tan Chok Shiong et al., 2006) (Hayato Shimizu et al., 2001) Some extended studies such as that airflow induces vibration in 3.5 HDD (Albert Tan Chok Shiong et al, 2006) and particle trajectory in HDD were reported. In this study, the author focuses on the 1.8-in HDD available in the market with the rotational speed of 3600 rpm, thus the Reynolds number based on the disk tip radius is around 12.6×10^3 . This paper describes the airflow investigation using the RNG k - ϵ turbulence model which is the most appropriate and economical turbulence model (H.Song et al, 2003) for HDD. The continuous investigation is the particle trajectory using the Stochastic Tracking Approach (Discrete Random Walk model).

NUMERICAL MODEL

The 3-D numerical model as shown in Fig.1 is constructed based on an actual 1.8-in hard disk drive inside the consumer products available in the market. The finite element methodology is used to carry out the

¹Student, Department of Mechanical Engineering, Faculty of Engineering, Khon Kaen University

²Assistant Professor, Department of Mechanical Engineering, Faculty of Engineering, Khon Kaen University

simulation, 1.2 million tetrahedral elements are used for all volume meshing. The Reynolds number based on disk tip radius is $Re = \omega r^2 = 12.6 \times 10^4$ where ω is the angular disk velocity, r is the disk radius and ν is the kinematic viscosity. The steady state simulation using RNG $k-\epsilon$ turbulence model is preferred in this study due to faster calculation when compared to the Reynolds Stress Model (RSM) (H.Song et al., 2003). Also, the RNG $k-\epsilon$ turbulence model gives more accuracy compared to the standard $k-\epsilon$ (H.Song et al., 2003). Hence, the RNG $k-\epsilon$ turbulence model employed in this study is robust and provides a general trend of the air flow inside the 1.8 in HDD with an acceptable calculation time.

The particle trajectory study has been performed after the flow study was finished. The Stochastic Tracking Approach using the Discrete Random Walk model has been employed to study the particle trajectory. Although this methodology gives us a zig-zag particle track, it is suitable to study the general particle trajectory in the flow field of a hard disk drive.

In order to make the flow field realistic, the recirculation filter was modeled using the porous jump model as the boundary condition. Also, setting the boundary condition of the recirculation filter was used as a “trap” to study performance of the recirculation filter; whether it is possible to catch the particles.

First of all, the models were constructed in order to investigate the air flow when the actuator arm functions at different positions: ID, MD and OD. Figure 2 shows schematic views of 1.8-in HDD when the actuator arm is at ID: Inner Diameter, MD: Middle Diameter and OD: Outer Diameter.

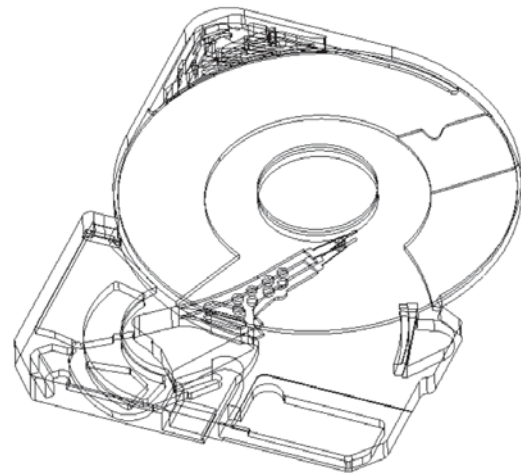
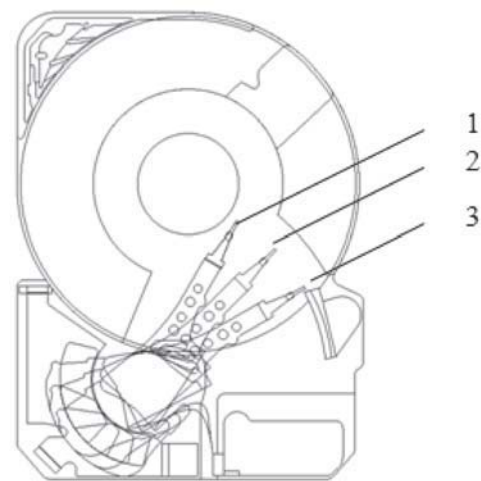


Figure 1. 3-D model of 1.8-in HDD available in the market.



1- Actuator arm at ID; 2-Actuator arm at MD;
3- Actuator arm at OD

Figure 2. Schematic view of 1.8-in HDD when the actuator arm is at ID, MD and OD.

RESULTS AND DISCUSSION

Simulation results provide many different flow variables values (e.g. static pressure, velocity). To study flow pattern in the hard disk drive, the velocity and static pressure are the main variables to analyze.

The particle trajectory assists the observation of the flow pattern in the HDD. The velocity plot at the recirculation filter shows how the porous jump model works.

Static Pressure Study in Hard Disk Drive

At the media surface, a comparison of pressure acting on the media surface at each arm position is as shown in Figure 3. At ID, we observe the arm's profile on the static pressure on the media; the highest pressure is close to the outside radius of the media. The arm's profile of static pressure seems to be reduced at MD and OD positions. Instead, the pressure acting on the leading edge of the slider is higher at the OD position. The maximum and minimum pressure observed in the model is around 18.4 Pascal and -14.6 Pascal respectively.

We observed similarly for all actuator arm positions ID, MD and OD that there is a negative pressure at the centre of the media. The pressure increases relatively with the increasing media radius. Also an increase in pressure is observed at the rim of the media where the ramp load is located as seen at the bottom left of the picture. This phenomenon is caused by the presence of the ramp load structure emerging into the rotating region.

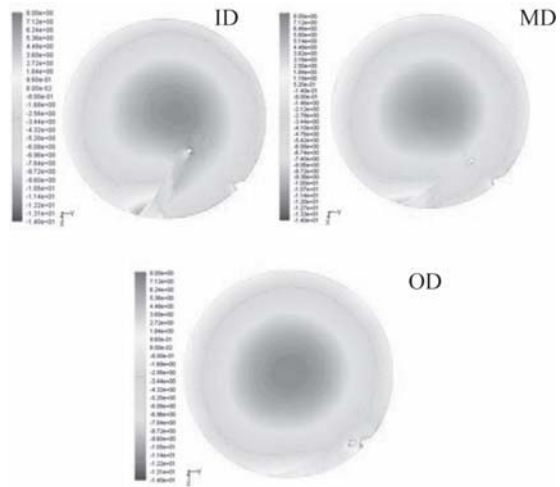


Figure 3. Contour plots of static pressure on the media surface when the actuator arm is at ID, MD and OD.

At the X-Y plane of $z = -0.5$ mm from the top cover, the surface cuts through arm 2, as shown in Figure 4. Simulation results shown higher pressure in the upstream region of the actuator arm especially when the actuator arm is at the ID position since air flow has been obstructed by the actuator arm. This effect decreases when the head moves out to MD and OD in order.

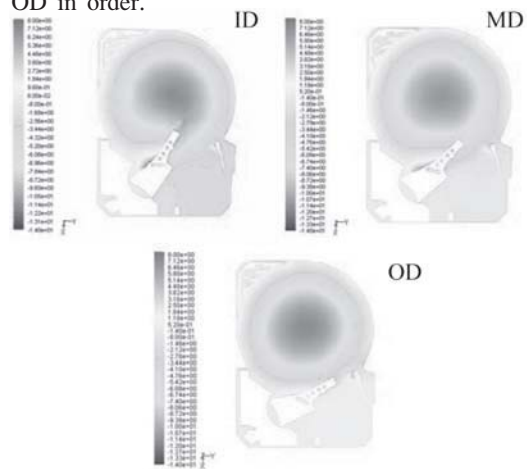


Figure 4. Contour plot of static pressure plot of X-Y plane at $Z = -0.5$ mm from the top when the actuator arm is at ID, MD and O

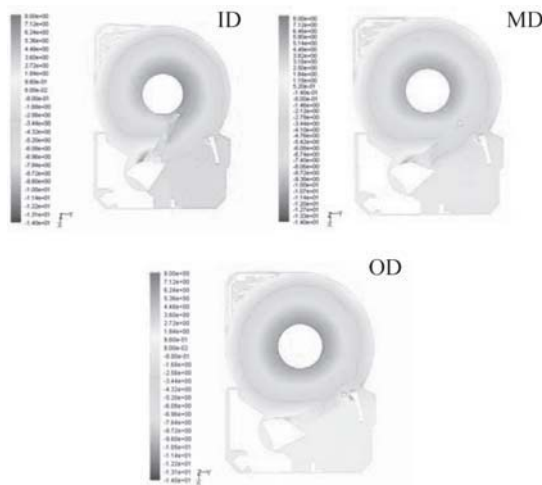


Figure 5. Contour plot of static pressure of X-Y plane at Z = -0.9 mm from the top when the actuator arm is at ID, MD and OD.

At the X-Y plane of z = -2 mm from the top cover, the surface cuts through the slider of arm 1, as shown in Figure 6. The impact from the base deck geometry on the pressure is more obvious. It is observed that the pressure pattern follows the base deck geometry. Again, higher pressure is acting on the upstream side of the slider when the head is at the OD position.

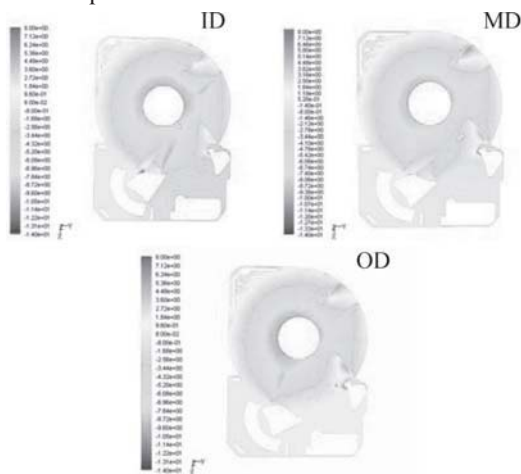


Figure 6. Contour plot of static pressure of X-Y plane at Z = -2.0 mm from the top when the actuator arm is at ID, MD and OD.

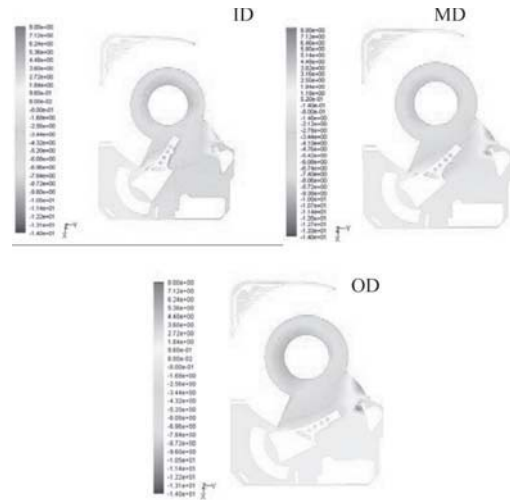


Figure 7. Contour plot of static pressure of X-Y plane at Z = -2.5 mm from the top when the actuator arm is at ID, MD and OD.

Velocity Study in Hard Disk Drive

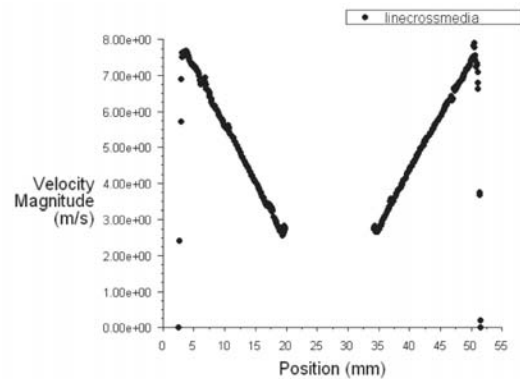


Figure 8. Plot of velocity magnitude across the media

The velocity of the air close to the disk surface shows a strong relationship with the linear velocity which increases corresponding to increasing disk radius according to the formula $v = \omega r$, as shown in Figure 8.

Air is obstructed by the slider, inducing a lower air velocity both upstream and downstream of the slider region. The presence of the ramp load structure emerging into the rotating disk region as seen in the lower left corner of the disk disperses the

wind direction, as shown in Figure 9.

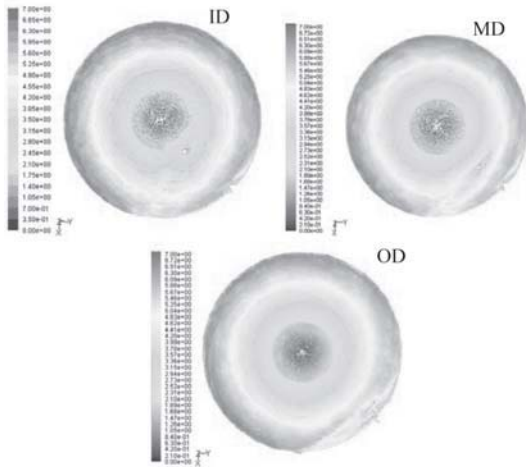


Figure 9. Vector plot of velocity on media surface when the actuator arm is at ID, MD and OD.

At the level of the X-Y plane at $z = 0.5$, the surface cuts through arm 2, and the air flow is obviously obstructed by the actuator arm when the actuator arm is at ID. The air velocity is thus reduced both upstream and downstream of the actuator arm, with the lower air velocity in the downstream region shown by the blue color close to the arm tip. The flow obstruction is reduced when the actuator arm moves to MD and OD. The flow pattern looks close to that of a spinning disk without the actuator arm when the actuator arm is at extreme OD.

Moreover, the results show the impact of the ramp load structure which emerges into the rotating disk region, since the air in the rotating disk region has been thrown downward when it hits the ramp load structure. When the actuator is at OD, the velocity of the air at the outer radius is maximized. The impact of this obstruction at OD is more obvious than when the actuator arm is at MD or ID. However, the air which is thrown downward by the ramp load structure will be evacuated back into the rotating disk region eventually (see Figure 9, 10 and 11). This

phenomenon creates the eddy at the bottom left outside the rotating disk, with the eddy diameter proportional to the actuator position.

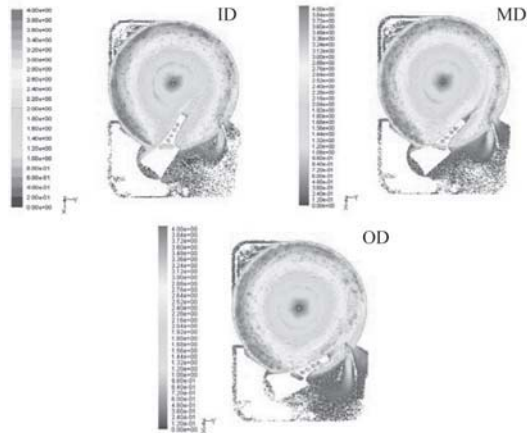


Figure 10. Vector plot of the air velocity of the X-Y plane at $Z = -0.5$ mm from the top when the actuator arm is at ID, MD and OD

At $z = -2$ mm (see Figure 12), we still see the impact of the base deck geometry on the velocity as well as at $z = -2.5$ mm. We observe a higher air velocity at the shallower region than the air velocity at the deeper region. At this z -level, we see the same flow pattern which is impacted by the ramp load as at the previous z -level.

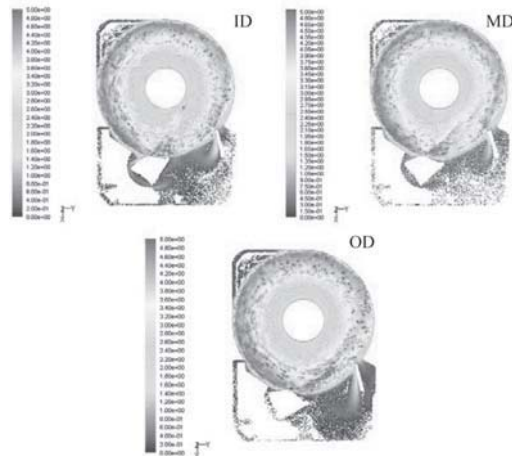


Figure 11. Vector plot of the air velocity of the X-Y plane at $Z = -0.9$ mm from the top when the actuator arm is at ID, MD and OD.

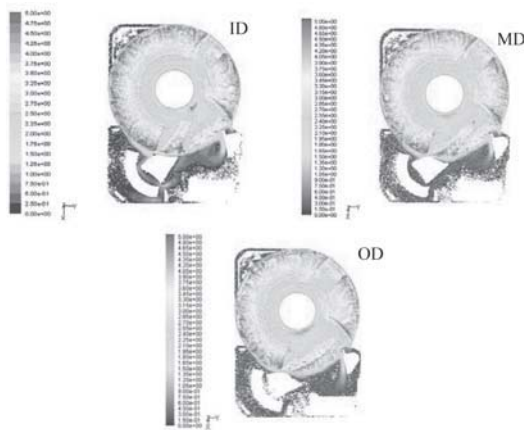


Figure 12. Vector plot of the air velocity of the X-Y plane at $Z = -2.0$ mm from the top when the actuator arm is at ID, MD and OD.

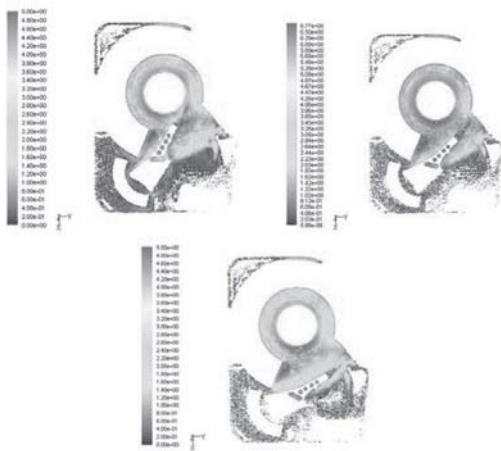


Figure 13. Vector plot of the air velocity of the X-Y plane at $Z = -2.5$ mm from the top when the actuator arm is at ID, MD and OD.

Study of air flow pattern and particle trajectory.

The study of particle trajectory assists with the observation of the air flow pattern in the hard disk drive.

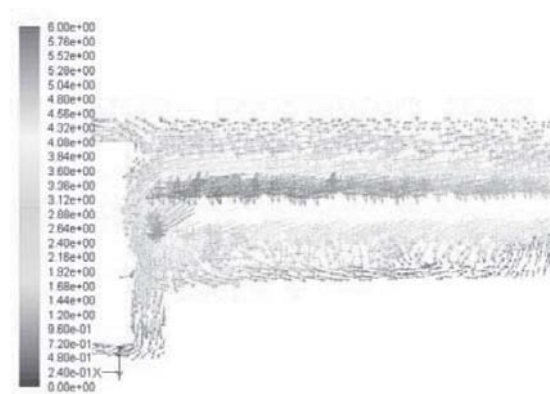


Figure 14. Velocity plot of the Z-X plane at the middle of the HDD showing that the air velocity above the rotating disk is higher than below the rotating disk.

To study the general particle trajectory in the hard disk drive, particles were released from the top of the HSA bearing which is considered to be the position that creates the particles because of the HSA screw tightening the HSA to the top cover of the hard disk drive. The size of the particles was set to $0.5 \mu\text{-inch}$. There were 3 tries in order to see as many as possible of the trajectories.

The result shows that the particles will be suddenly evacuated into the center of the rotating disk in a spiral form, then the particles are thrown outward from the center to the disk.

Particles sometimes detour to the voice coil, Flex and PCC connector. Eventually, the air will be evacuated into the rotating disk region again. Also, the whirlpool at the ramp load area creates particle movement like a spiral.

The flow pattern in a 1.8 in HDD resulting from the numerical model shows air flow with the high velocity following the solid body rotation (media). Some of the air has been thrown outside the rotating

disk and slowly moves along the recirculation filter before it is evacuated back to the rotating disk region. When the air reaches the actuator arm, it will be thrown out from the left hand side of the HDD. Then the air passes slowly through the complex geometry of the HSA and Voice Coil Magnet, Flex and PCC connector. Eventually, air will be evacuated into the rotating disk region again at the right hand side of the HDD at the region close to the ramp load area.

The air in the rotating disk region flows with higher velocity with maximum velocity at the OD region. The numerical results show that the velocity of the air above the disk surface is higher than the air below the disk surface. The difference in velocity between the upper and lower portions of the rotating disk results from the non-symmetrical nature of the volume above and below the rotating disk, as seen in Figure 14. Also, the density of the particle trajectory above the disk surface is higher than below the disk surface as shown in Figure 16.

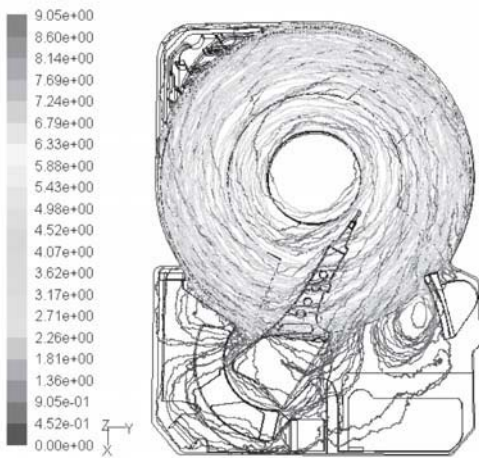


Figure 15. Particle Trajectory of 5 trial discreet random walk model showing general particle tracking in the hard disk drive.

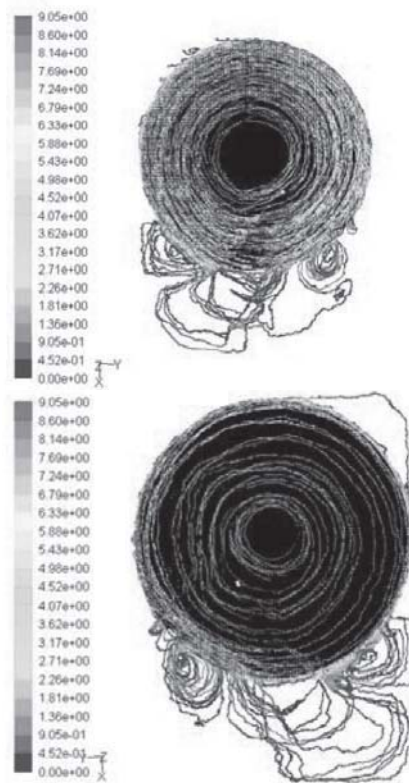


Figure 16. Particle Trajectory above the rotating disk (left) has higher density than particle trajectory below the rotating disk.

CONCLUSION

The steady state air flow inside a 1.8 in HDD has been simulated using the RNG $k-\epsilon$ turbulence model which gives more accurate results than the standard $k-\epsilon$ turbulence model while consuming less time than the RSM.

The numerical results show a greater value of pressure acting on the actuator arm body when the actuator arm is at ID, especially at the upstream region of the actuator as well as the pressure acting on the media. In contrast, the pressure at the slider increases when the actuator arm moves from ID to OD.

The velocity in the rotating disk area increases linearly along the disk surface from ID to OD. The

air is obstructed by the actuator arm especially when the actuator arm is at ID. The ramp load emerging into the rotating disk area changes the direction of the air to move downward before it is evacuated back into the rotating region; the more the actuator arm moves to OD the greater the value of velocity of the air which is thrown downward.

Particle motion in the hard disk drive happens mostly in the upper portion of the rotating disk because of the higher velocity of the air. Particles which were released from the HSA bearing were evacuated into the rotating disk area. Sometimes, particles detour around the coil side with low velocity. The whirlpool at the ramp load area creates particle movement like a spiral.

REFERENCES

- M.A. Suriadi, C.S. Tan, Q.D. Zhang, T.H. Yip, K, Sundaravadivelu. "Numerical investigation of airflow inside a 1-in hard disk drive" **Journal of Magnetism and Magnetic Materials** 303 (2006) e124 - e127.
- H.Song, M. Damodaran and Quock Y. Ng. "Simulation of Flow Field and Particle Trajectories in Hard Disk Drive Enclosure" **Seagate Technology International** 2003.
- Albert Tan Chok Shiong, Maria, Aanastasia Suriadi and Zhang Qide. "Studies on Air Flow Induced Vibration in a Simplified Hard Disk Drive using LES" **Magnetic and Recording Asia Pacific** 2006.
- Hayato Shimizu, Mikio Tokuyama, Satomitsu Imai, Shigeo Nakamura, and Kazuo Sakai, "Study of Aerodynamic Characteristics in Hard Disk Drives by Numerical Simulation" **IEEE TRANSACTIONS ON MAGNETICS**, VOL. 37, NO. 2, MARCH 2001.